WELDING RESEARCH

SUPPLEMENT TO THE *WELDING JOURNAL*, APRIL 2004
Sponsored by the American Welding Society and the Welding Research Council

Liquation Cracking in Full-Penetration Al-Mg-Si Welds

A higher fraction solid in the weld metal than in the partially melted zone during terminal solidification is a necessary condition for cracking to occur

BY C. HUANG AND S. KOU

ABSTRACT. Liquation cracking in the partially melted zone (PMZ) of full-penetration welds of Alloy 6061 (Al-1Mg-0.6Si) was investigated. The PMZ is the region outside the fusion zone where grain-boundary liquation occurs during welding. Circular-patch welds of Alloy 6061 were made by gas metal arc welding with both filler metals 5356 (Al-5Mg) and, 4043 (Al-5Si), and the dilution was about 66%. Liquation cracking occurred with 5356 but not 4043. Curves of temperature (T) vs. fraction solid (f_S) were calculated for 1) the PMZ (same as the base metal) of Alloy 6061 and its welds made with filler metals 5356 and 4043, and 2) the PMZ of Alloy 6082 (Al-0.7Mg-0.9Si) and its welds made with filler metals NG61 (similar to 5356) and NG21 (similar to 4043). Various dilution levels were covered. All curves were based on the multicomponent Scheil model and temperature-dependent equilibrium partition ratio k and liquidus slope m_L. They were compared with the experimental results in the present study on 6061, in Metzger's study on 6061 (Ref. 3), and in Gittos and Scott's study on 6082 (Ref. 5). It was found that weld metal f_S > PMZ f_S during PMZ terminal solidification in welds that liquation cracked, and that weld metal f_S < PMZ f_S throughout PMZ solidification in welds that didn't crack. Therefore, the following is a necessary condition for liquation cracking to occur: The weld metal that is solidifying, contracting, and pulling the PMZ must have a higher f_S (or more precisely, a higher strength) than the PMZ during PMZ terminal solidification. This condition is more realistic than that of Gittos and Scott based on the equilibrium solidus temperature because nonequilibrium solidification, which prevails in welding, can be considered through f_S. This condition was applied to liquation cracking in: 1) full-penetration Al-Mg-Si welds, including explaining the well-known opposite effects of 5356 and 4043 on liquation cracking; 2) multipass Al-Mg-Si welds of thick plates, where the dilution is lower than that in full-penetration welds (sheet material); and 3) full-penetration Al-Cu welds, as well.

C. HUANG and S. KOU are respectively Graduate Student and Professor in the Department of Materials Science and Engineering, University of Wisconsin, Madison, Wis.

Introduction

Aluminum alloys are known to be susceptible to liquation cracking. Liquation and liquation cracking in aluminum welds have received much attention (Refs. 1–20). They occur in the partially melted zone (PMZ) — the region immediately outside the fusion zone where the material is heated above the eutectic temperature (or above the solidus temperature if the workpiece is solutionized before welding) (Ref. 1). Liquation occurs along the grain boundary as well as in the grain interior. Because of grain-boundary liquation, cracking can occur along grain boundaries under tensile strains during welding. Significant tensile strains are induced in the workpiece when it is restrained and unable to contract freely upon cooling during welding.

The weld metal composition is determined by the base-metal composition, the filler-metal composition and the dilution ratio. The dilution ratio herein refers to the extent the filler metal is diluted by the base metal that melts and forms the weld with the filler metal.

KEY WORDS

Aluminum
Alloy 6061
Alloy 6082
Liquation Cracking
Partially Melted Zone
Circular-Patch Test
Scheil Equation

Metzger (Ref. 3) observed liquation cracking in full-penetration, gas tungsten arc (GTA) welds of Alloy 6061 (essentially Al-1Mg-0.6Si) made with Al-Mg filler metals at high dilution ratios, but not in similar welds made with Al-Si filler metals at any dilution ratio. Specifically, liquation cracking was observed in welds of composition Al-1.6Mg-0.5Si made with an Al-3Mg filler metal at a dilution ratio of about 76%, and in welds of composition Al-1.9Mg-0.5Si made with an Al-5Mg filler metal at about the same dilution ratio. No cracking was observed in the following 6061 welds: Al-3.2Mg-0.3Si made with an Al-5Mg filler metal at 44% dilution, Al-0.8Mg-1.5Si made with an Al-5Si filler metal at 78% dilution, and Al-0.6Mg-3.2Si made with an Al-5Si filler metal at 45% dilution.

Gittos and Scott (Ref. 5) conducted the circular-patch test (Ref. 21) on Alloy 6082 (essentially Al-0.7Mg-0.9Si). Full-penetration GTA welds were made with filler metals NG61 (essentially Al-5.2Mg, close to 5356) and NG21 (essentially Al-5Si, close to 4043). It was concluded that "liquation cracking occurred when using NG61 filler metal with base metal dilutions of ~ 80%" and "cracking did not occur when using NG21 filler metal." Specifically, liquation cracking was observed in welds containing from 1.3 to 1.8% Mg and 0.7 to 0.8% Si made with NG61 at a dilution ratio ranging from about 77 to 88%. (No dilution ratios outside this range were reported.) No cracking was observed in a weld of composition Al-0.6Mg-1.8Si made with NG21 at a dilution ratio of 78%. (No other dilution ratios were shown.) It was suggested that liquation cracking occurs if the weld-metal

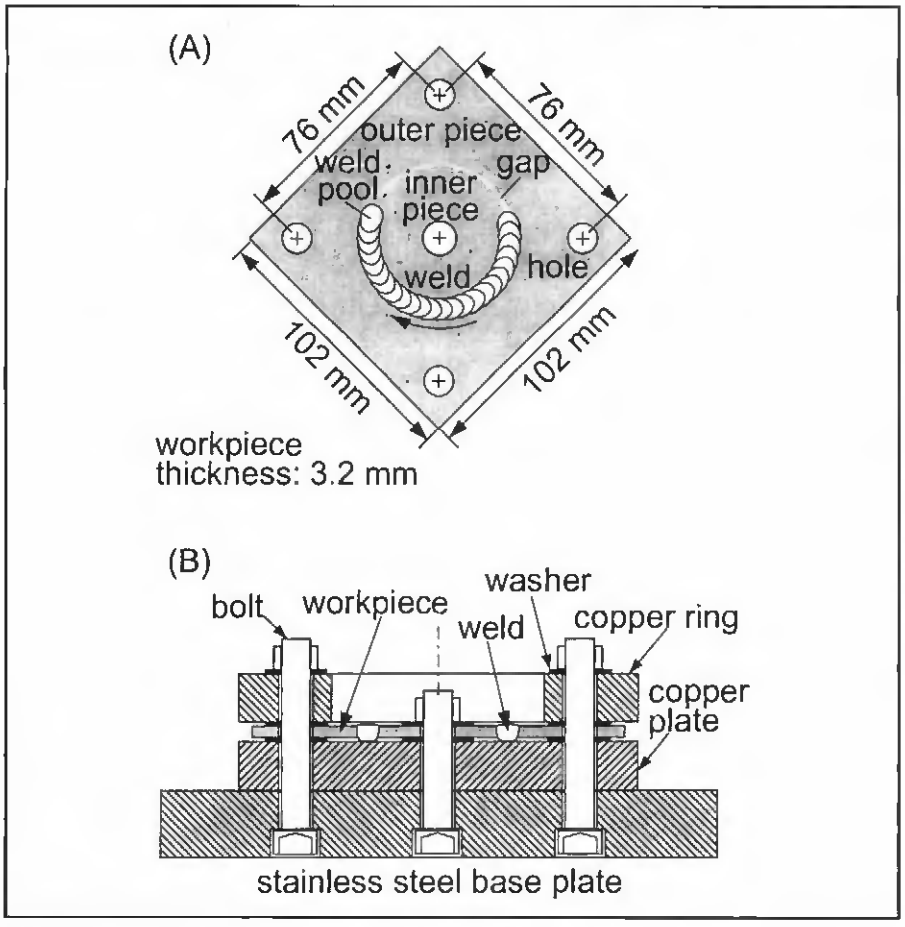

Fig. 1 — Circular-patch test. A — Top view of workpiece; B — side view of apparatus.

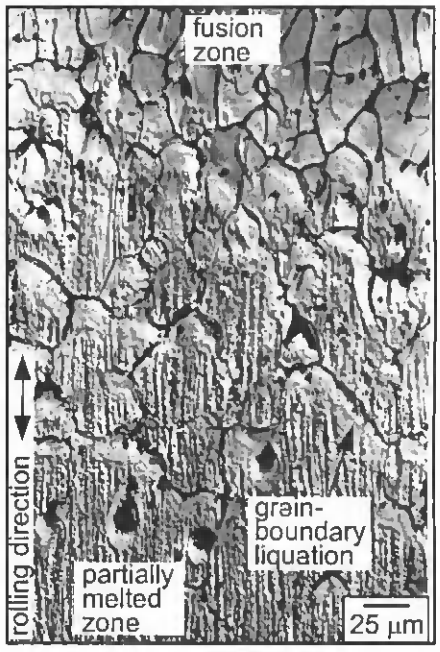

Fig. 2 — Evidence of significant liquation along grain boundaries in partially melted zone of Alloy 6061.

solidus temperature is higher than the base-metal solidus temperature.

Katoh et al. (Ref. 7), Kerr et al. (Ref. 8), and Miyazaki et al. (Ref. 9) investigated the effect of weld-metal composition on liquation cracking in welds of 6000-series aluminum alloys including Alloy 6061. They used the Varestraint test (Refs. 22, 23) to evaluate the susceptibility to liquation cracking. Partial-penetration welds were made by GTAW and GMAW (gas metal arc welding). Longitudinal liquation cracking occurred when Alloy 6061 was welded with filler metal 5356 but not with filler metal 4043. Contrary to Gittos and Scott (Ref. 5), however, Miyazaki et al. (Ref. 9) found that the weld-metal solidus temperature was lower than the base-metal solidus temperature (597°C) regardless of whether the filler metal was 5356 or 4043. It was suggested that the Alloy 6061 probably liquated at 559°C by constitutional liquation induced by the Al-Mg_2Si-Si ternary eutectic.

Huang and Kou (Ref. 24) studied liquation cracking in partial-penetration aluminum welds of Alloy 2219 made with filler metals 1100, 2319, 4047, 4145, and 2319 plus extra Cu. It was discovered that the papillary- (nipple-) type penetration common in GMAW with spray transfer tends to oscillate along the weld and promote liquation cracking near the weld root regardless of the filler metal used. The resultant weld root was wavy along the welding direction, and cracking occurred mostly in the areas between waves. The deformation of the grains and cracks in the PMZ near the weld root suggested that the solidifying and contracting weld metal pulled the liquated PMZ near the weld root and caused cracking. A mechanism was proposed to explain the effect of penetration oscillation on liquation cracking near the weld root.

Huang, Cao, and Kou (Ref. 25) investigated liquation cracking in partial-penetration aluminum welds of Alloys 2024, 6061, and 7075. Filler metals 1100 and 4043 were used. Papillary penetration and wavy weld roots were observed in all welds. With either filler metal, severe liquation and liquation cracking occurred in Alloys 2024 and 7075 but not in Alloy 6061, where liquation was light and no liquation cracking occurred.

Huang and Kou (Ref. 26) also studied liquation cracking in full-penetration welds of Alloy 2219, which was selected because it is a simple binary Al-6.3Cu alloy. Circular-patch welds of Alloy 2219 were made by GMAW with filler metals of various Cu contents. The curves of temperature vs. fraction solid were calculated for both the PMZ and the weld metal from the Scheil equation without a computer code because only binary Al-Cu alloys were involved. The curves were essentially parallel to one another *without* any intersections and they showed that, in the welds that liquation-cracked, the weld metal fraction solid exceeded the PMZ fraction solid *throughout* PMZ solidification. It was observed that near solidification cracks liquation cracking either tended to stop or not to occur at all.

Cross and Gutscher (Ref. 27) studied the effect of Cu and Fe content on the solidification cracking and PMZ liquation in Alloy 2519. The circular-patch test was used.

In the present study, liquation cracking in full-penetration welds of Alloy 6061 is investigated using the circular-patch test. The curves of temperature vs. fraction solid, which are *complicated and intersect* one another, are calculated for Alloys 6061 and 6082 and their welds, based on the Scheil model for multicomponent alloys and using *a computer code and database*. They are used to explain liquation cracking in the present study and the studies of Metzger (Ref. 3), and Gittos and Scott (Ref. 5).

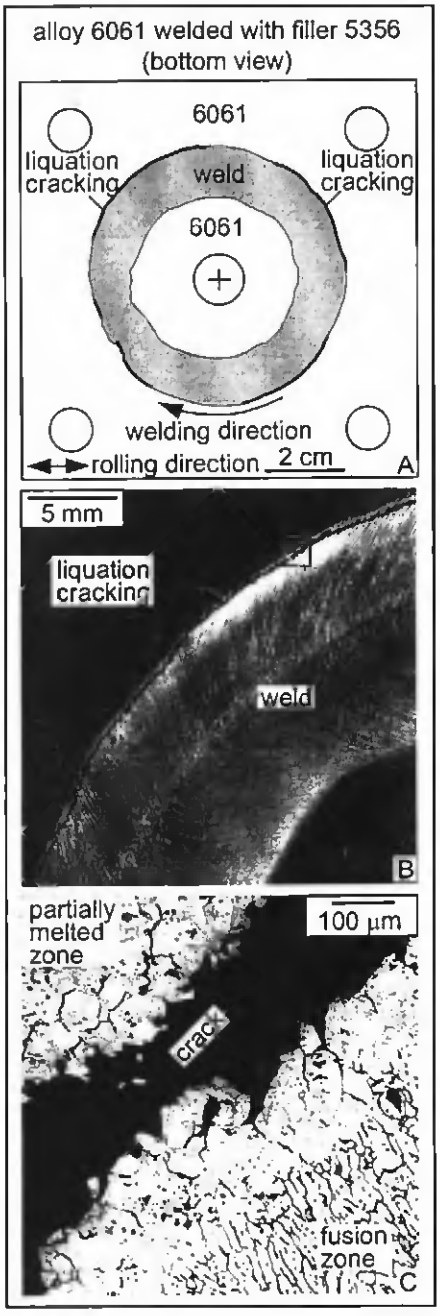

Fig. 3 — Weld of Alloy 6061 made with filler metal 5356. A — Overview; B — macrograph; C — micrograph of area in square in B. Bottom surface of weld.

Table 1 — Compositions of Workpiece and Filler Metals in wt-% (balance: Al)

	Mg	Si	Cu	Mn	Zn	Ti	Cr	Fe
				Workpiece				
6061	0.91	0.68	0.23	0.07	0.05	0.05	0.19	0.44
6082 sheet 1	0.63	0.91	0.04	0.530	0.02	0.03	0.008	0.32
6082 sheet 2	0.72	0.94	0.03	0.51	0.02	0.04	0.005	0.34
6082 average	0.675	0.925	0.035	0.52	0.02	0.035	0.0065	0.33
				Filler Metals				
4043	0.05	5.20	0.30	0.05	0.10	0.20	—	0.8
5356	5.00	0.25	0.10	0.05	0.10	0.06	0.05	0.4
NG 61	5.25	0.20	0.10	0.80	0.10	0.05–0.20	0.05–0.20	0.2
NG 21	0.20	5.25	0.10	0.50	0.20	—	—	<0.6

Compositions of 6082, NG 21, and NG 61 taken from Gittos and Scott (Ref. 5).

Experimental Procedure

The circular-patch test (Ref. 21) was used to evaluate the susceptibility to liquation cracking, as shown in Fig. 1. In order to prevent the workpiece from contracting freely during welding, the workpiece was highly restrained by being bolted down to a thick stainless steel plate. The workpiece for circular-patch welding is shown in Fig. 1A. It consisted of an outer piece and an inner piece, and both were Alloy 6061. The filler metal was either 4043 or 5356. Alloy 6061 was welded in the as-received condition of T6. The actual compositions of the workpiece and the filler metals are listed in Table 1.

The joint design was a square butt joint in 3.2-mm-thick material with a 0.25-mm root opening. The outer piece had an 11.1-mm-diameter hole in each corner, and the inner piece (circular patch) had a hole of 12.7 mm at the center.

The fixture for circular-patch welding is shown in Fig. 1B. The outer piece was sandwiched between a copper plate (152 × 152 × 19 mm) at the bottom and a copper ring (19 mm thick, 83 mm ID, and 152 mm × 152 mm on the outside) at the top. The workpiece, together with the copper plate and the copper ring, was bolted down to a stainless steel base plate of 203 × 203 × 25.4 mm. The bolts were tightened with a torque wrench to the same torque of 47.5 m-N to ensure consistent restraint conditions. A similar design was used by Nelson et al. (Ref. 28) for assessing solidification cracking in steel welds.

The workpiece was separated from the copper plate and the copper ring by steel washers 1.6 mm thick, 12.2 mm ID, and 23.5 mm OD. Without the washers, it was difficult to make full-penetration welds because of the heat-sink effect of copper. Welding was conducted by the gas metal arc welding (GMAW) process with electrode-positive polarity (DCEP) and with argon as the shielding gas. The inner and outer pieces were not tack welded prior to GMAW. Since the pieces were held down tightly, there was no problem keeping the pieces flat due to distortion during welding. The distance between the contact tube and workpiece was about 25.4 mm, and the welding gun was perpendicular to the workpiece. The welding speed was 4.2 mm/s (based on a 1.6 rpm rotation speed and a 51 mm diameter). The filler metal was 1.2 mm in diameter and was positioned at 25.4 mm from the center of the workpiece. With filler metal 4043, the wire feed rate was 93 mm/s, the average current 140 A, and the voltage 22 V. With filler metal 5356, however, the arc was less stable, the average welding current was significantly lower, and spattering of filler-metal droplets was observed. These resulted in a weld narrower than what was needed to achieve about the same dilution ratio as in the weld made with filler metal 4043. Consequently, the wire feed rate and the voltage were raised to 106 mm/s and 24 V, respectively, in order to raise the average welding current to 125 A. The power (voltage times current) was 3080 W in the case of 4043 and 3000 W in the case of 5356, which were very close to each other.

The weld surface was cleaned with a solution of 48 vol-% HF in water. Macrographs of the welds were taken with a digital camera. The welds were then sectioned and etched with Keller's reagent. The weld microstructure was examined with an optical microscope.

Houldcroft (Ref. 29) reported that the composition of a single-pass GMA aluminum weld is essentially uniform. This is because the Lorenz force, surface-tension gradients, and droplet impingement all help mix the filler metal with the melted base metal (Ref. 1).

It is assumed that the Mg loss due to the high-Mg vapor pressure is not significant enough to change the weld metal composition. The concentration of any element, E, in the weld metal was calculated as follows (Ref. 1):

$$\%\ E \text{ in weld metal} = (\%\ E \text{ in base metal}) \times [A_b / (A_b + A_f)] + (\%\ E \text{ in filler metal}) \times [A_f / (A_b + A_f)] \quad (1)$$

where A_b and A_f are the areas in the weld transverse cross section that represent contributions from the base metal and the

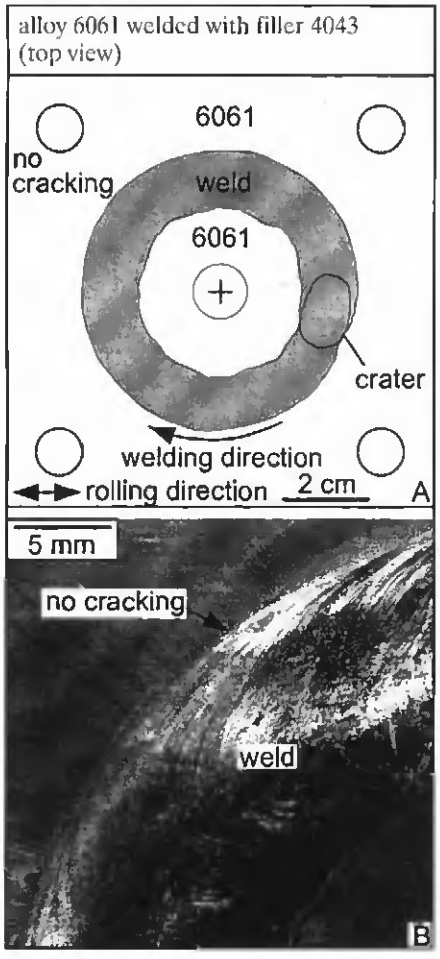

Fig. 4 — Weld of Alloy 6061 made with filler metal 4043. A — Overview; B — macrograph. Top surface of weld.

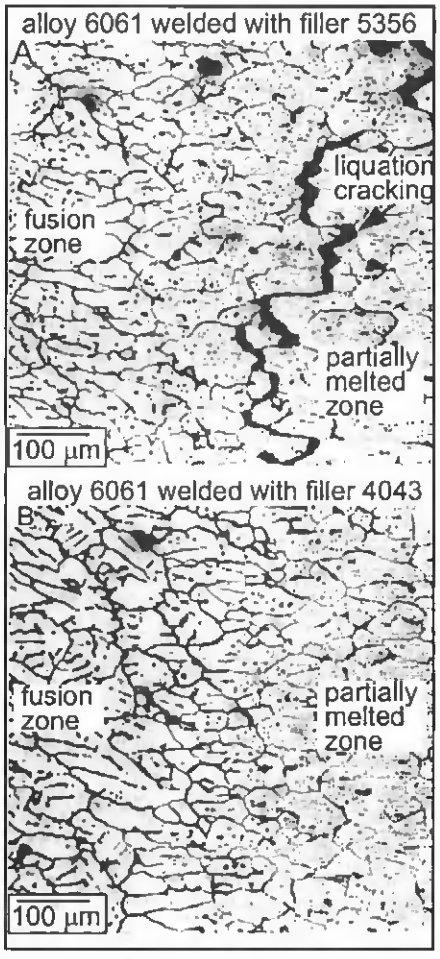

Fig. 5 — Transverse cross sections of welds of Alloy 6061 made with filler metals. A — 5356; B — 4043.

Table 2 — Weld-Metal Dilution Ratios and Compositions in wt-% (balance: Al)

Weld (workpiece/ filler metal)	Dilution Ratio (%)	Mg	Si	Cu	Mn	Zn
6061/5356	64.1	2.376	0.526	0.183	0.063	0.068
6061/4043	67.6	0.631	2.146	0.253	0.064	0.066

filler metal, respectively. The ratio $A_b/(A_b + A_f)$ is the dilution ratio. The transverse macrograph of the weld was taken with a digital camera and enlarged on the computer monitor. The cross-sectional areas of the entire weld A_1, the face reinforcement A_2, and the root reinforcement A_3 were selected and calculated using commercial computer software. From these data, areas A_b and A_f were determined, that is, $A_b = A_1 - (A_2 + A_3)$ and $A_f = A_2 + A_3$.

Results and Discussion

For convenience, all welds are identified by two numbers, the first referring to the workpiece and the second the filler metal. For instance, weld 6061/5356 refers to the weld made in Alloy 6061 with a filler metal of Alloy 5356. The measured dilution ratios of the welds are shown in Table 2.

Evidence of Grain-Boundary Liquation

Significant liquation was observed in the PMZ of the welds. Figure 2 is a micrograph showing the transverse cross section of weld 6061/4043. It was taken with DIC (differential interference contrast) to better reveal the liquated and re-solidified material along the grain boundaries in the PMZ. The lines in the PMZ along the rolling direction were rolling bands. The eutectic at grain boundaries and the α phase next to them are clear evidence that significant grain-boundary liquation occurred in the PMZ during welding. During cooling, the grain-boundary liquid (hypoeutectic) solidified first into the solute-depleted α phase and finally as the solute-rich eutectic at grain boundaries. Huang and Kou (Refs. 16–20) studied grain-boundary liquation and the resultant grain-boundary segregation in several aluminum alloys including 6061 (Ref. 18).

6061 Welded with Filler Metal 5356

As shown in Table 2, the weld metal composition of weld 6061/5356 was essentially Al-2.38Mg-0.53Si (dilution ratio 64.1%). Because of the high vapor pressure of Mg caused by filler metal 5356 (essentially Al-5Mg), some filler metal droplets from spattering landed on the top surface of the weld (Ref. 30). Consequently, the bottom surface of the weld instead of the top surface was examined for liquation cracking. Figure 3A is the overview of the bottom of the weld traced from the digital photograph of the weld with the help of computer software. The cracks were marked with thick lines for clarity. Such an overview was used instead of the photograph itself because cracks were too small to see at the magnification of the overview.

As shown in Fig. 3A, liquation cracking was severe, extending along more than half (59%) of the outer edge of the weld. Liquation cracking occurred along the outer edge of the weld but not the inner edge, as evident from the macrograph taken from the upper-left region of the weld and shown in Fig. 3B. The solidification shrinkage of aluminum is as high as 6.6% (Ref. 31), and the thermal expansion coefficient of aluminum is roughly twice that of iron-based alloys. Therefore, aluminum alloys have a tendency to contract significantly during solidification. Since the apparatus (Fig. 1) kept the workpiece from contracting, the outer edge of the weld was in tension while the inner edge was in compression. Consequently, liquation cracking occurred only along the outer edge of the weld. Figure 3C shows the microstructure inside the small square in Fig. 3B. The liquated PMZ looked clearly different from the cellular/dendritic structure of the fusion zone.

6061 Welded with Filler Metal 4043

As shown in Table 2, the weld metal composition of weld 6061/4043 was essentially Al-0.63Mg-2.15Si (dilution ratio 67.6%). Figure 4A shows the overview of the top of the weld, including the crater (which is visible from the top) at the termination of welding. As shown, there was

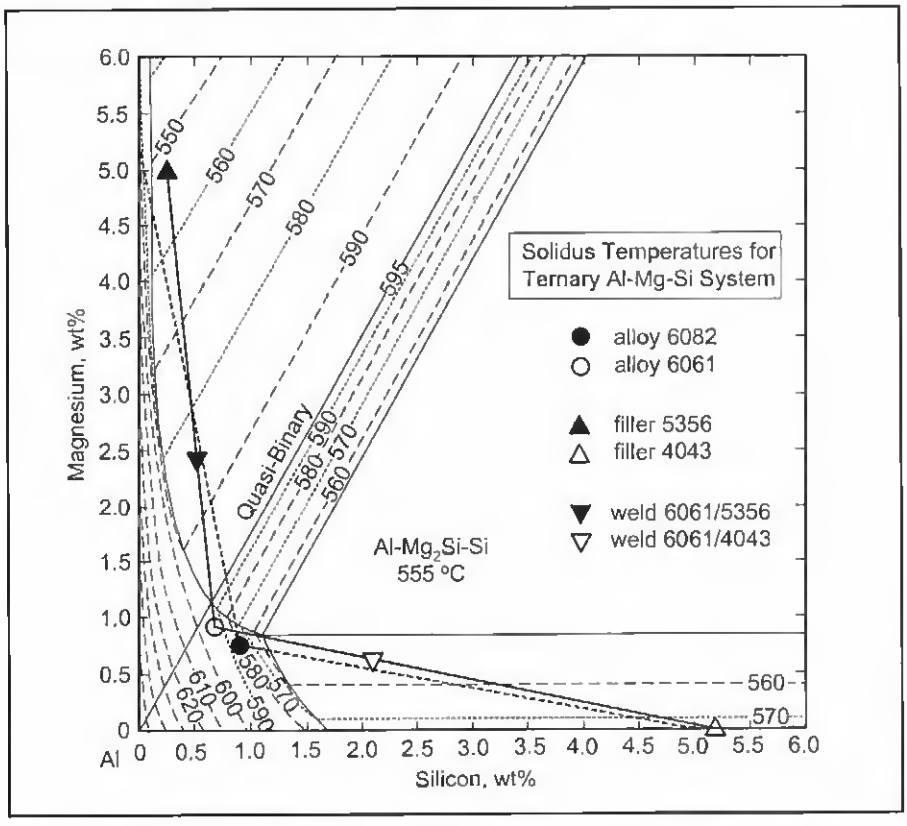

Fig. 6 — Locations of alloys, filler metals, and weld metals on solidus-temperature map of ternary Al-Mg-Si system.

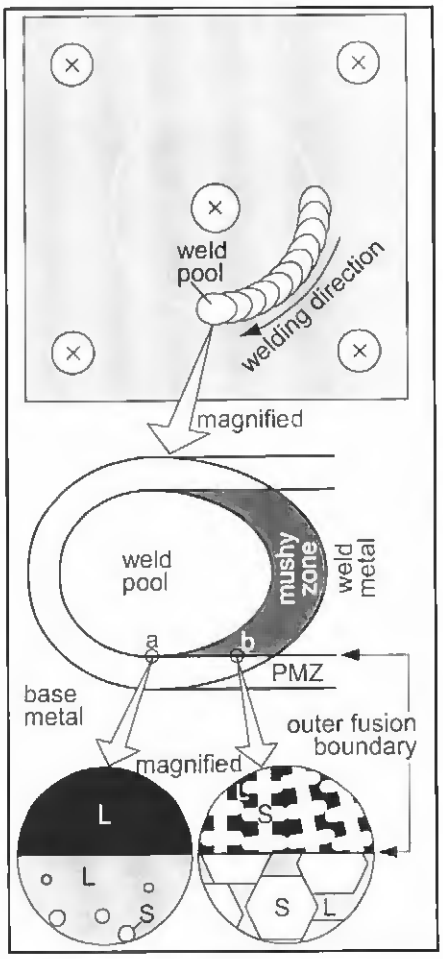

Fig. 7 — Schematic sketch of microstructure at fusion boundary during welding. PMZ, partially melted zone; S, solid; L, liquid.

no liquation cracking in this weld. The macrograph in Fig. 4B, taken from the upper left region of the weld, confirms the absence of liquation cracking.

Figure 5 shows the transverse cross sections of welds 6061/5356 and 6061/4043. Figure 5A was taken from an area in weld 6061/5356 where the liquation cracks were very fine, in order to better reveal the intergranular feature of liquation cracking. No liquation cracking was visible in weld 6061/4043, as shown in Fig. 5B.

Liquation Cracking and Solidus Temperatures

Figure 6 shows a map of the solidus temperatures (T_S) in the Al-rich corner of the ternary Al-Mg-Si system (Ref. 32), which Gittos and Scott (Ref. 5) used to explain liquation cracking in Alloy 6082. They pointed out that the weld-metal T_S relative to the base-metal T_S has a significant effect on liquation cracking. Alloy 6082 (essentially Al-0.7Mg-0.9Si) has a T_S of 580°C. With filler metal Al-5.2Mg, the weld-metal T_S varies along the thick dotted line from 6082 to Al-5.2Mg, passing through a maximum temperature of 595°C. At high dilution ratios, that is, at a short distance along the dotted line from the 6082, weld-metal T_S > base-metal T_S. With filler metal Al-5Si, the weld-metal T_S varies along the thick dotted line from 6082 to Al-5Si, decreasing first and then increasing somewhat but always staying below the base-metal T_S of 580°C.

In other words, for Alloy 6082 welded with Al-5.2Mg at high dilution ratios, weld-metal T_S > base-metal T_S, and liquation cracking did occur. For Alloy 6082 welded with Al-5Si at any dilution ratios, on the other hand, weld-metal T_S < base-metal T_S, and liquation cracking did not occur. In light of these relationships between T_S and liquation cracking, Gittos and Scott (Ref. 5) stated, "The proposed mechanism of HAZ cracking is that, during welding, grain boundary melting occurs in the HAZ and with certain base metal and weld metal compositions, it is possible for the base metal solidus to be below the weld metal solidus. Thus, when tensile strains arising from weld metal solidification are imposed on the HAZ, cracking occurs at such boundaries."

Alloy 6061 (essentially Al-0.91Mg-0.68Si) and its welds in the present study are also included in Fig. 6. For weld 6061/4043 (essentially Al-0.63Mg-2.15Si), the weld-metal T_S of about 557°C is lower than the base-metal T_S of about 595°C. Liquation cracking did not occur (Fig. 4) and this is consistent with Gittos and Scott (Ref. 5). For weld 6061/5356 (essentially Al-2.38Mg-0.53Si), on the other hand, the weld-metal T_S of about 585°C is also lower than the base-metal T_S of about 595°C. However, liquation cracking occurred (Fig. 3), contrary to Gittos and Scott (Ref. 5).

Since the cooling rate during welding is relatively high, the equilibrium solidification condition that the solidus temperature represents, in fact, does not exist in welding. Nonequilibrium solidification, instead, will be considered as stated below.

Curves of Temperature vs. Fraction Solid

Instead of using the solidus temperatures like Gittos and Scott (Ref. 5), Huang and Kou (Ref. 26) used the fraction solid to assess the potential for liquation cracking to occur in a binary Al-Cu Alloy 2219. Figure 7 shows schematically the microstructure at fusion boundary during circular-patch welding. As shown, at the fusion boundary in area *a*, the weld metal and the PMZ are both in the liquid state (L). At the fusion boundary in area *b*, both the weld

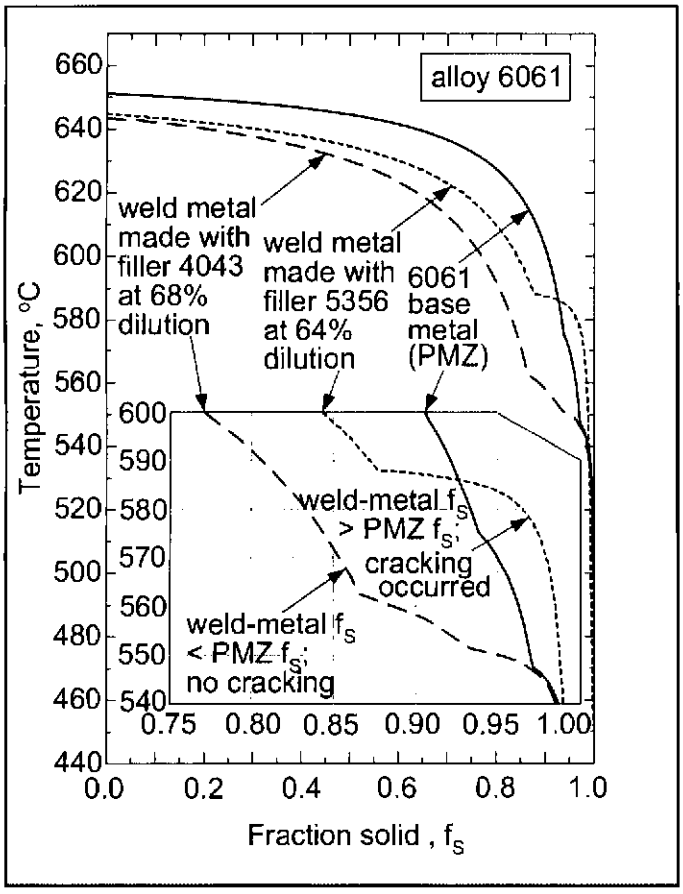

Fig. 8 — T vs. f_S curves for 6061 and its welds made in the present study. With filler 5356 at 64% dilution, liquation cracking occurred and weld-metal f_S > PMZ f_S during PMZ terminal solidification. With 4043 at 68% dilution, liquation cracking did not occur and weld-metal f_S < PMZ f_S. Curves were calculated using Pandat *of CompuTherm LLC (Ref. 33).*

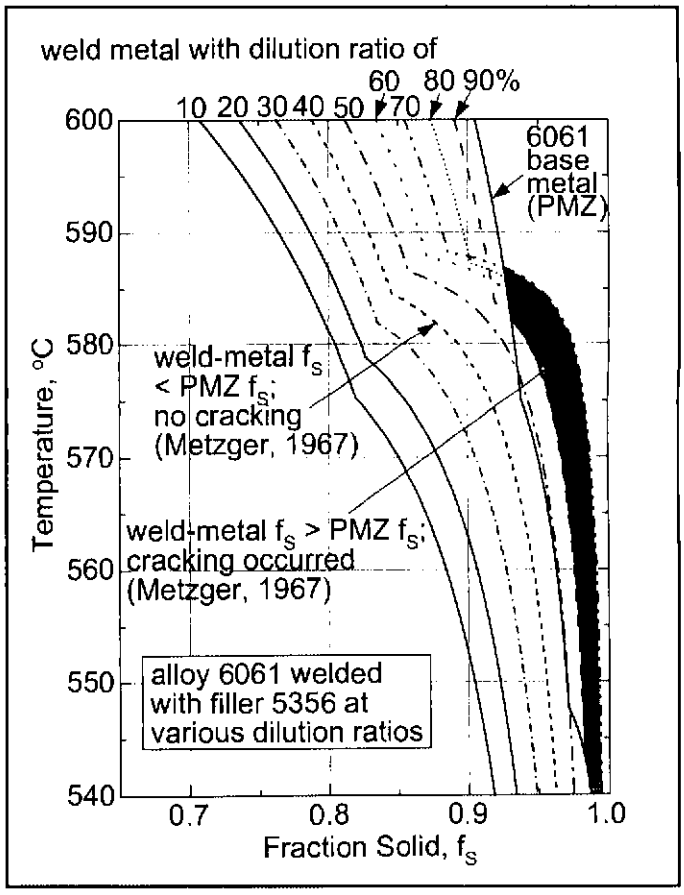

Fig. 9 — T vs. f_S curves for 6061 and its welds made with filler metal 5356. Weld-metal f_S > PMZ f_S at 60–90% dilution (shaded area), which includes the weld metals Al-1.6Mg-0.5Si and Al-1.9Mg-0.5Si that caused liquation cracking. Weld-metal f_S < PMZ f_S at 40% dilution, which is close to the weld metal Al-3.2Mg-0.3Si that caused no cracking. Curves were calculated using Pandat *of CompuTherm LLC (Ref. 33).*

metal and the PMZ have been solidifying and thus are in the semisolid state (S + L).

The fraction solid of a semisolid formed during nonequilibrium solidification can be calculated by using the Scheil equation (Ref. 1), which is based on the assumptions of complete diffusion in liquid, no diffusion in solid, and equilibrium between solid and liquid at the solid/liquid interface. As an approximation, the fraction solid f_S at any given temperature T can be calculated from the following Scheil equation:

$$f_S = 1 - \left(\frac{T_m - T_L}{T_m - T} \right)^{\frac{1}{1-K}} \qquad (2)$$

where T_m is the melting point of pure aluminum, T_L the liquidus temperature of the alloy, and k the equilibrium partition ratio. This simple form of the Scheil equation is based on the assumptions that the solidus line and the liquidus line of the binary phase diagram are both straight lines, that is, the equilibrium partition ratio and the slope of the liquidus line are both constant. It can be shown (Ref. 1) that the Scheil equation can also be written as

$$f_S = 1 - \left(\frac{(-m_L)C_0}{T_m - T} \right)^{\frac{1}{1-k}} \qquad (3)$$

where m_L (< 0) is the slope of the liquidus line in the phase diagram and C_0 is the solute content of the alloy before solidification.

For multicomponent alloys, the fraction solid must be calculated numerically because Equations 2 and 3 are for binary alloys only. A computer code *Pandat* was used, which is a software package for calculating multicomponent phase diagrams, solidification paths, and thermodynamic properties (Ref. 33). A database *PanAluminum* was also used, which is a thermodynamic database for aluminum alloys based on the experimental data of thermodynamic properties and phase equilibria (Ref. 34). The software and the database have been tested extensively against binary and multicomponent aluminum alloys (Refs. 35–51). All thermodynamic models are built in *Pandat*, and all model parameters are listed in the database. In the computation of the phase diagram, the compositions of the solid and liquid phases at each temperature are calculated, based on which k and m_L at each temperature are calculated, that is, they are both temperature dependent. No special equation forms are needed, such as sums of polynomials.

For the present study, the following six components were selected from *PanAluminum*: Al, Cu, Mg, Mn, Si, and Zn. Elements Cr, Ti, and Fe were neglected. These elements are not associated with liquation in Alloy 6061 (Ref. 18). The Scheil model for multicomponent alloys was used as an approximation, but with temperature-dependent k and m_L. More advanced solidification models can be used to calculate the fraction solid more accurately than the Scheil model if necessary.

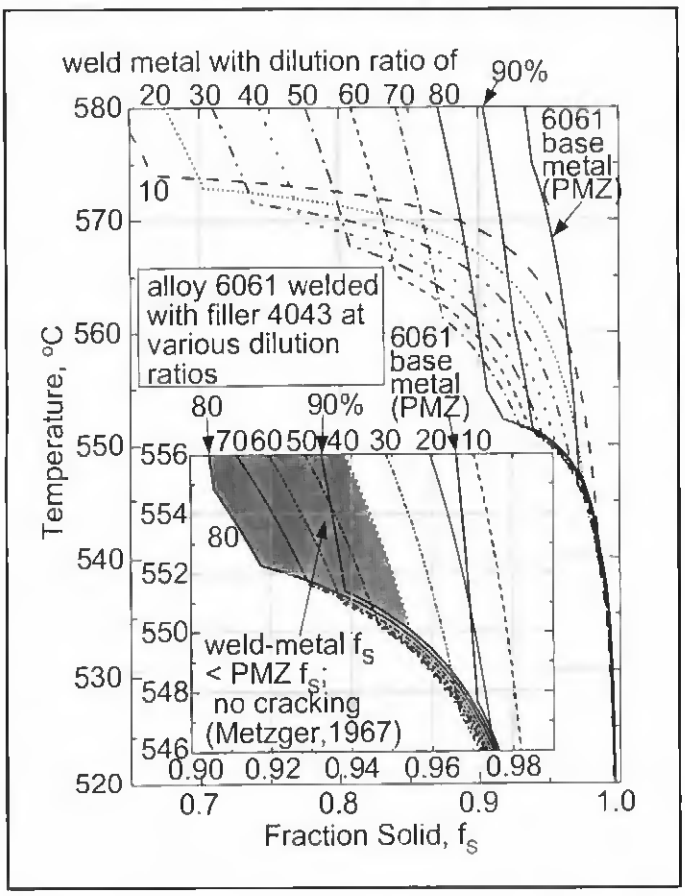

Fig. 10 — T vs. f_S curves for 6061 and its welds made with filler 4043. Weld-metal f_S < PMZ f_S at 40–90% dilution (shaded area), which includes the weld metals Al-0.8Mg-1.5Si and Al-0.6Mg-3.2Si that caused no cracking. Curves were calculated using Pandat *of CompuTherm LLC (Ref. 33).*

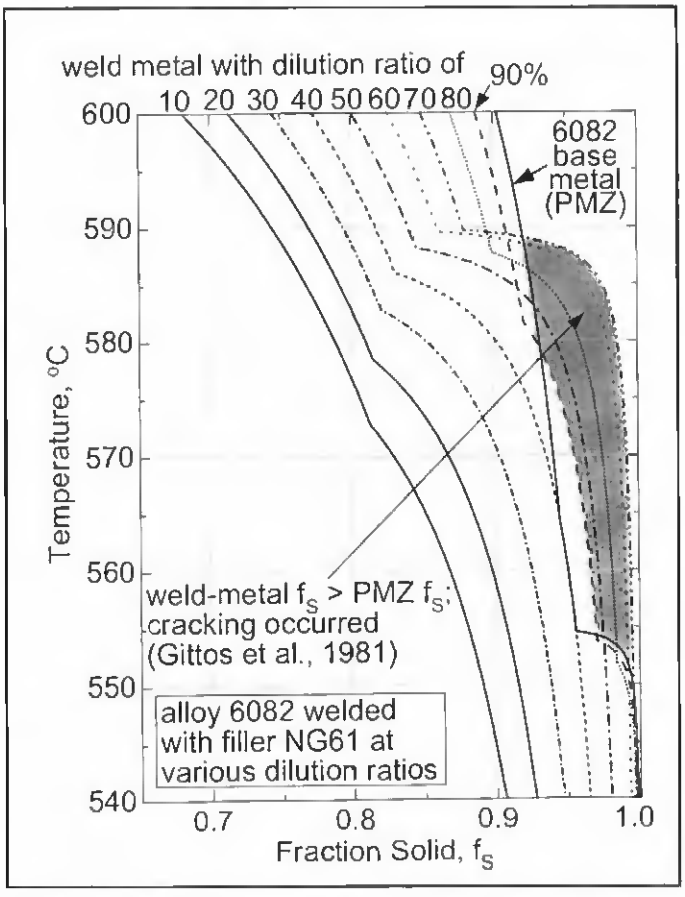

Fig. 11 — T vs. f_S curves for 6082 and its welds made with filler NG61. Weld-metal f_S > PMZ f_S at 70–90% dilution (shaded area), which includes the weld metals Al-(1.3–1.8)Mg-(0.7-0.8)Si that caused liquation cracking. Curves were calculated using Pandat *of CompuTherm LLC (Ref. 33).*

Comparing T-f_S Curves with Welds in Present Study

Figure 8 shows the weld-metal and PMZ T-f_S curves of welds 6061/4043 and 6061/5356. The starting end of a T-f_S curve at $f_S = 0$ corresponds to the onset of formation of the primary Al phase (α) from the liquid. For Alloy 6061 PMZ solidification is essentially over, i.e., $f_s = 0.99$, at 537°C. Consider arbitrarily the last 40°C before that as PMZ terminal solidification. A portion of the curves during terminal solidification is enlarged for clarity. A kink appears in a T-f_S curve when a secondary phase starts to form with α simultaneously from the liquid, that is, when the liquidus slope changes due to intersection with a line of twofold saturation, such as a eutectic valley. For instance, in the curve for the PMZ of Alloy 6061, the first kink at 575°C corresponds to the onset of simultaneous formation of Mg_2Si and α, and the second kink at 547°C to the onset of simultaneous formation of the Si-rich phase and α. It is assumed that the secondary phase will nucleate as soon as such a valley is reached, that is, without significant undercooling.

It is evident from Fig. 8 that there are interesting things happening below the aforementioned base-metal solidus temperature of about 595°C. Consider the curve for weld 6061/5356. The kink at about 588°C corresponds to the onset of simultaneous formation of Mg_2Si and α. At 595°C the weld-metal f_S is lower than the PMZ f_S but it increases sharply at about 588°C. From about 585° to 540°C the weld-metal f_S becomes higher than the PMZ f_S. This shows that the weld metal becomes higher in f_S than the PMZ during PMZ terminal solidification.

Consider the curve for weld 6061/4043 now. At 595°C the weld-metal f_S is much lower than the PMZ f_S. The kink at about 563°C corresponds to the onset of the simultaneous formation of the Si-rich phase and α from the liquid, and that at about 552°C, to the onset of the simultaneous formation of Mg_2Si with α. Although f_S increases with decreasing temperature, it remains lower than the PMZ f_S during PMZ terminal solidification. Thus, the weld metal remains lower in f_S than the PMZ throughout PMZ solidification.

Therefore, the T-f_S curves for the welds in the present study show that liquation cracking occurs when weld-metal f_S > PMZ f_S during PMZ terminal solidification, but not when weld-metal f_S < PMZ f_S throughout PMZ solidification.

Comparing T-f_S Curves with Welds in Metzger's Study

Figure 9 shows the T-f_S curves for the PMZ (base metal) and weld metal of Alloy 6061 made with filler metal 5356 at dilution ratios ranging from 10 to 90%. The compositions of the weld metal are listed in Table 3. As shown by the shaded area in Fig. 9, the weld-metal T-f_S curve clearly crosses over the PMZ T-f_S curve at the dilution ratios of 60 to 90%, with the maxi-

Table 3 — Weld-Metal Dilution Ratios and Compositions (in wt-%) in the Case of Alloy 6061 Welded with Filler Metal 5356

Dilution Ratio (%)	Mg	Si	Cu	Mn	Zn	Al
10	4.591	0.293	0.113	0.052	0.095	94.856
20	4.182	0.336	0.126	0.054	0.090	95.212
30	3.773	0.379	0.139	0.056	0.085	95.568
40	3.364	0.422	0.152	0.058	0.080	95.924
50	2.955	0.465	0.165	0.060	0.075	96.280
60	2.546	0.508	0.178	0.062	0.070	96.636
70	2.137	0.551	0.191	0.064	0.065	96.992
80	1.728	0.594	0.204	0.066	0.060	97.348
90	1.319	0.637	0.217	0.068	0.055	97.704

Table 4 — Weld-Metal Dilution Ratios and Compositions (in wt-%) in the Case of Alloy 6061 Welded with Filler Metal 4043

Dilution Ratio (%)	Mg	Si	Cu	Mn	Zn	Al
10	0.136	4.748	0.293	0.052	0.095	94.676
20	0.222	4.296	0.286	0.054	0.090	95.052
30	0.308	3.844	0.279	0.056	0.085	95.428
40	0.394	3.392	0.272	0.058	0.080	95.804
50	0.480	2.940	0.265	0.060	0.075	96.180
60	0.566	2.488	0.258	0.062	0.070	96.556
70	0.652	2.036	0.251	0.064	0.065	96.932
80	0.738	1.548	0.244	0.066	0.060	97.308
90	0.824	1.132	0.237	0.068	0.055	97.684

Table 5 — Weld-Metal Dilution Ratios and Compositions (in wt-%) in the Case of Alloy 6082 Welded with Filler Metal NG61

Dilution Ratio (%)	Mg	Si	Cu	Mn	Zn	Al
10	4.7925	0.2725	0.0935	0.772	0.182	93.8875
20	4.3350	0.3450	0.0870	0.744	0.164	94.3250
30	3.8775	0.4175	0.0805	0.716	0.146	94.7625
40	3.4200	0.4900	0.0740	0.688	0.128	95.2000
50	2.9625	0.5625	0.0675	0.660	0.110	95.6375
60	2.5050	0.6350	0.0610	0.632	0.092	96.0750
70	2.0475	0.7075	0.0545	0.604	0.074	96.5125
80	1.5900	0.7800	0.0480	0.576	0.056	96.9500
90	1.1325	0.8525	0.0415	0.548	0.038	97.3875

Table 6 — Weld-Metal Dilution Ratios and Compositions (in wt-%) in the Case of Alloy 6082 Welded with Filler Metal NG21

Dilution Ratio (%)	Mg	Si	Cu	Mn	Zn	Al
10	0.2475	4.8175	0.0935	0.502	0.182	94.1575
20	0.2950	4.3850	0.0870	0.504	0.164	94.5650
30	0.3425	3.9525	0.0805	0.506	0.146	94.9725
40	0.3900	3.5200	0.0740	0.508	0.128	95.3800
50	0.4375	3.0875	0.0675	0.510	0.110	95.7875
60	0.4850	2.6550	0.0610	0.512	0.092	96.1950
70	0.5325	2.2225	0.0545	0.514	0.074	96.6025
80	0.5800	1.7900	0.0480	0.516	0.056	97.0100
90	0.6275	1.3575	0.0415	0.518	0.038	97.4175

mum crossover occurring at about 70% dilution. As shown in Table 3, this range of dilution ratio corresponds to the composition range of 1.3 to 2.5% Mg and 0.5 to 0.6% Si.

As mentioned previously, Metzger (Ref. 3) observed liquation cracking in welds of composition Al-1.6Mg-0.5Si made with an Al-3Mg filler metal at a dilution ratio of about 76%, and in welds of composition Al-1.9Mg-0.5Si made with an Al-5Mg filler metal at about the same dilution ratio. These welds are essentially in between the 60%-dilution weld (Al-2.5Mg-0.5Si) and the 90%-dilution weld (Al-1.3Mg-0.6Si) in Table 3. According to Fig. 9, weld-metal f_S > PMZ f_S during PMZ terminal solidification, about 45°C at 60% dilution and 40°C at 90%.

Metzger (Ref. 3) found no cracking in welds of composition Al-3.2Mg-0.3Si made with an Al-5Mg filler metal at a dilution ratio of about 44%. These welds are close in composition to the 40%-dilution weld (Al-3.4Mg-0.4Si) in Table 3. According to Fig. 9, weld-metal f_S < PMZ f_S throughout PMZ solidification.

Figure 10 shows the T-f_S curves for the PMZ (base metal) and weld metal of Alloy 6061 made with filler metal 4043 at dilution ratios ranging from 10 to 90%. The compositions of the weld metal are listed in Table 4. As shown in Fig. 10, the weld metal T-f_S curve does not crossover the PMZ T-f_S curve except at 10–20% dilution.

Metzger (Ref. 3) observed no cracking in welds of composition Al-0.8Mg-1.5Si made with an Al-5Si filler metal at a dilution ratio of about 78%. He also observed no cracking in welds of composition Al-0.6Mg-3.2Si made with an Al-5Si filler metal at a dilution ratio of about 45%. These welds are essentially in between the 40%-dilution weld (Al-0.4Mg-3.4Si) and the 90%-dilution weld (Al-0.8Mg-1.1Si) in Table 4. As shown by the shaded area in Fig. 10, weld-metal f_S < PMZ f_S throughout PMZ solidification.

Therefore, the T-f_S curves for the welds in Metzger's study (Ref. 3) also show that liquation cracking occurs when weld-metal f_S > PMZ f_S during PMZ terminal solidification, but not when weld-metal f_S < PMZ f_S throughout PMZ solidification.

Comparing T-f_S Curves with Welds in Gittos' Study

For Alloy 6082 PMZ solidification is essentially over, i.e., f_S = 0.99, at 552°C. Consider again arbitrarily the last 40°C before that as PMZ terminal solidification. Figure 11 shows the T-f_S curves for the PMZ (base metal) and weld metal of Alloy 6082 made with filler metal NG61 (Al-5.25Mg-0.4Si) at dilution ratios ranging from 10 to 90%. The

compositions of the weld metal are listed in Table 5. As shown in Fig. 11, the weld-metal T-f_S curve clearly crosses over the PMZ T-f_S curve at the dilution ratios of 50 to 90%, with the maximum crossover occurring at about 70% dilution.

Gittos and Scott (Ref. 5) observed liquation cracking in welds containing from 1.3 to 1.8% Mg and 0.7 to 0.8% Si made with a NG61filler metal at a dilution ratio ranging from about 77 to 88%. These welds are between the 70%-dilution weld (Al-2.0Mg-0.7Si) and the 90%-dilution weld (Al-1.1Mg-0.9Si) in Table 5. As shown by the shaded area in Fig. 11, for these welds weld metal f_S > PMZ f_S during PMZ terminal solidification.

Figure 12 shows the T-f_S curves for the PMZ (base metal) and weld metal of Alloy 6082 made with filler metal NG21 (Al-0.2Mg-5.25Si) at dilution ratios ranging from 10 to 90%. The compositions of the weld metal are listed in Table 6. As shown in Fig. 12, the weld-metal T-f_S curve crosses over the PMZ T-f_S curve at 10% and 20% dilution.

Gittos and Scott (Ref. 5) found no cracking in a weld of composition Al-0.6Mg-1.8Si made with a NG21 filler metal at a dilution ratio of 78%. This weld is close in composition to the 80%-dilution weld (Al-0.6Mg-1.8Si) in Table 6. According to Fig. 12, weld-metal f_S < PMZ f_S throughout PMZ solidification.

Therefore, the T-f_S curves for the welds in the study of Gittos and Scott (Ref. 5) also show that liquation cracking occurs when weld-metal f_S > PMZ f_S during PMZ terminal solidification, but not when weld-metal f_S < PMZ f_S throughout PMZ solidification.

Necessary Condition for Liquation Cracking Based on Fraction Solid

The mechanism of liquation cracking in full-penetration aluminum welds has been described in the study on Al-Cu welds by Huang and Kou (Ref. 26) as follows. Liquation cracking is caused by the tensile strains induced in the PMZ by the solidifying and contracting weld metal that exceed the PMZ resistance to cracking. This requires a combination of significant tensile strains in the PMZ and a susceptible PMZ microstructure, both of which have already been described (Ref. 26). In brief, significant tensile strains exist in the PMZ if 1) the workpiece has a tendency to contract significantly (such as aluminum alloys welded under significant heat inputs) but is kept from contracting freely by the restraint imposed on it, 2) the weld metal is higher in strength than the PMZ during solidification to force the PMZ to accommodate the contraction strains, and 3) there is no solidification cracking in the weld metal to relax the tensile strains in the nearby PMZ. Experimental data have shown that the strength of a semi-solid aluminum alloy increases with increasing solid fraction (decreasing temperature) (Ref. 52). As an approximation, the secondary effect of the microstructure and grain size on the strength will be neglected, and the strengths of the weld metal and the PMZ will be compared based on the fraction solid. A susceptible PMZ microstructure exists when there is sufficient liquation to weaken the PMZ significantly. A lightly liquated PMZ is resistant to cracking. For a given workpiece material, the tensile strains and liquation in the PMZ are both affected significantly by the welding condition.

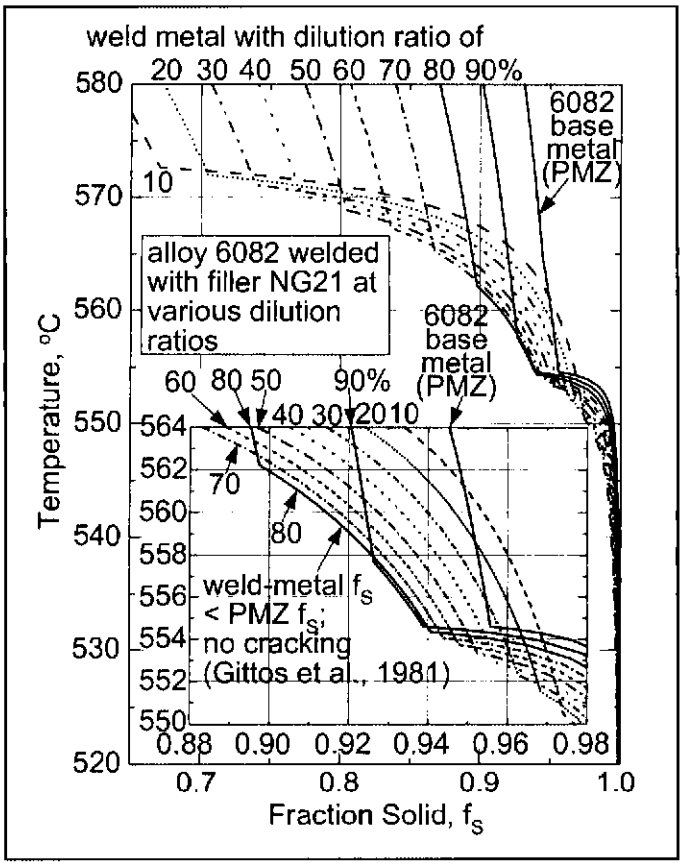

Fig. 12 — T vs. f_S curves for 6082 and its welds made with filler NG21. Weld-metal f_S < PMZ f_S at 80% dilution, which corresponds to the weld metal Al-0.6Mg-1.8Si that caused no liquation cracking. Curves were calculated using Pandat *of CompuTherm LLC (Ref. 33).*

It is, therefore, proposed that for liquation cracking to occur in full-penetration aluminum welds, the solidifying and contracting weld metal must have a higher fraction solid (or more precisely a higher strength) than the PMZ that it pulls during PMZ terminal solidification. This condition for liquation cracking is more realistic than that of Gittos and Scott (Ref. 5) based on the equilibrium solidus temperature because nonequilibrium solidification, which prevails in welding, can be considered through the fraction solid. Liquation cracking is not likely to occur in full-penetration welds when the weld metal is lower in fraction solid (or more precisely a lower strength) than the PMZ throughout PMZ solidification.

In addition to this condition, the workpiece must have a tendency to contract significantly during solidification. Furthermore, there must be significant restraint to keep the workpiece from contracting freely, significant liquation to weaken the PMZ, and no solidification cracking to relax the strains in the nearby PMZ. These additional conditions have been proposed by Huang and Kou (Ref. 26).

If the PMZ is higher in solid fraction and does not crack, the weld metal will have to accommodate high restraint. Whether the weld metal will crack depends on whether it is within the composition range that is susceptible to solidification cracking. Experimental data of the ternary Al-Mg-Si system (Ref. 53) show that Alloy 6061 (close to Al-1Mg-0.6Si) is highly susceptible to solidification cracking but much less so when welded with filler metal 4043 or 5356, especially the former. This suggests that the weld metal may not crack. Huang and Kou (Ref. 26) have shown in the case of Alloy 2219 (Al-6.3Cu) that raising the weld metal Cu content (e.g., to 3.4%) to eliminate liquation cracking can cause solidification cracking. However, both solidification cracking and liquation cracking disappeared when the Cu content was raised further (e.g., to 6.3%) to beyond the composition range most susceptible to solidification cracking (around 3% Cu).

Multipass Welds of Thick Plates

Liquation cracking in multipass welds of thick plates will be considered here.

The dilution ratios in the welds discussed above are about 66% in the circular-patch welds in the present study, 45–80% in the straight-line welds in Metzger's study (Ref. 3), and 75–90% in the circular-patch welds in the study of Gittos and Scott (Ref. 5). These dilution levels are appropriate for single-pass welds in sheet material.

In thick-section multipass welds typical dilution levels are in the range of 10–40%, which are also covered in the f_S-T curves in Figs. 9 through 12. At these lower dilution levels Al-Mg filler metals are much less likely to cause liquation cracking. In Fig. 9 the weld-metal f_S-T curves for the welds made with filler metal 5356 at 10–40% dilution do not cross over the PMZ curve of Alloy 6061. Similarly, in Fig. 11 the weld-metal f_S-T curves for the welds made with filler metal NG61 at 10–40% dilution do not cross over the PMZ curve of Alloy 6082.

Ellis et al. (Ref. 12) observed liquation cracking in 80-mm-thick plates of Alloy 6082 multipass welded with filler metal 5356 but not 4043. The dilution ratios were not measured but were said likely to be somewhat below 50%. It was noticed that liquation cracks were perpendicular to the fusion boundary and parallel to the rolling direction, instead of parallel to the weld interface as in the case of sheet material (Ref. 5). In view of this, it was suggested that bands of solute segregation through the plate thickness could have enhanced the local alloy content in the PMZ and caused liquation cracking at lower dilution levels than in thin material. A higher local alloy content (C_o) in the PMZ means a lower local f_S at a given temperature T, as can be seen from Equation 3 even though it is for binary alloys. Consequently, even at a relatively low dilution ratio, it is possible for weld-metal f_S > PMZ f_S to occur locally in the PMZ and cause liquation cracking along the bands of segregation.

Contrary to Al-Mg filler metals, Al-Si filler metals are more likely to cause liquation cracking at lower dilution levels, say, 10–40%, than at higher dilution levels, say, 50–90%. In Fig. 10 the weld-metal f_S-T curves for the welds made with filler metal 4043 at 10–20% dilution cross over the PMZ curve of Alloy 6061. Similarly, in Fig. 12 the weld-metal f_S-T curves for the welds made with filler metal NG21 at 10–30% dilution cross over the PMZ curve of Alloy 6082.

Al-Cu Welds

The necessary condition for liquation cracking in full-penetration Al-Cu welds is, in fact, a special case of the one proposed here for Al-Mg-Si welds. The T-f_S curves for Al-Cu welds are simple; they do not intersect one another, in fact, they are essentially parallel to one another. As shown by Huang and Kou (Ref. 26), a higher f_S (or more precisely a higher strength) in the weld metal than in the PMZ throughout PMZ solidification is a necessary condition for liquation cracking in Al-Cu welds. The condition proposed here for liquation cracking in Al-Mg-Si welds, in fact, also applies to Al-Cu welds. This is because weld metal f_S > PMZ f_S during PMZ terminal solidification includes the special case of weld-metal f_S > PMZ f_S throughout PMZ solidification.

Summary and Conclusions

The present study was conducted to investigate the well-known liquation-cracking phenomenon in full-penetration welds of 6000-series aluminum alloys and to explain the opposite effects of filler metals 5356 and 4043 on liquation cracking. The circular-patch test was used to evaluate the crack susceptibility. Full-penetration welds were made by GMAW with filler metals 5356 and 4043. The macrostructure and microstructure of the resultant welds were examined. Curves of temperature (T) vs. fraction solid (f_S) were calculated for both the PMZ and the weld metal to help understand liquation cracking by comparing the T-f_S curve of the weld metal against that of the PMZ.

The conclusions are as follows:

1) *Confirmation of Metzger's study*: The experimental results in the present study show that welding Alloy 6061 with filler metal 5356 at a high dilution ratio can cause liquation cracking but not with filler metal 4043. This is consistent with Metzger's experimental results on Alloy 6061 (Ref. 3).

2) *Contradiction to Gittos' theory*: Gittos and Scott (Ref. 5) proposed a liquation-cracking theory based on the equilibrium solidus temperature T_S, that is, liquation cracking occurs when weld-metal T_S > base-metal T_S. The use of T_S unfortunately prevented nonequilibrium solidification, which prevails in welding, from being considered. In the present study, filler metal 5356 caused liquation cracking in Alloy 6061 at 64% dilution. However, the T_S of the weld metal, 585°C, is less than the T_S of the base metal (same as PMZ), 595°C.

3) *T-f_S curves for Al-Mg-Si welds*: Based on the Scheil model for multicomponent alloys and the temperature-dependent equilibrium partition ratio k and liquidus slope m_L, T-f_S curves have been calculated for both the PMZ (same as base metal) and the weld metal. These curves, ranging from 10 to 90% dilution, include: Alloy 6061 welded with filler metals 5356 and 4043, and Alloy 6082 welded with filler metals NG61 (similar to 5356) and NG21 (similar to 4043). Unlike in the case of Al-Cu welds, where the T-f_S curves are simple and essentially parallel to one another, the T-f_S curves of Al-Mg-Si welds can be much more complicated and can intersect one another.

4) *T-f_S curves and liquation cracking in 6061*: When compared with the 6061 welds in the present study made with filler metals 5356 and 4043 and in Metzger's study (Ref. 3), the T-f_S curves show that weld-metal f_S > PMZ f_S during PMZ terminal solidification in the welds that cracked, and that weld-metal f_S < PMZ f_S throughout PMZ solidification in the welds that did not crack.

5) *T-f_S curves and liquation cracking in 6082*: When compared with the 6082 welds made with filler metals NG61 and NG21 by Gittos and Scott (Ref. 5), the T-f_S curves also show that weld metal f_S > PMZ f_S during PMZ terminal solidification in the welds that cracked, and that weld-metal f_S < PMZ f_S throughout PMZ solidification in the welds that did not crack.

6) *Necessary condition for liquation cracking in Al-Mg-Si welds*: For liquation cracking to occur in full-penetration welds, there must be a higher fraction solid (or more precisely, a higher strength) in the weld metal than in the PMZ during PMZ terminal solidification. Since this condition is based on f_S instead of T_S, nonequilibrium solidification can be considered, either through the basic Scheil model or more advanced solidification models that can predict T-f_S curves more accurately than the Scheil model. In addition, there must be 1) a significant tendency for the workpiece to contract during solidification, 2) significant restraint to keep the workpiece from contracting freely, 3) significant liquation to weaken the PMZ, and 4) no solidification cracking nearby to relax the strains in the PMZ. Liquation cracking is not likely to occur in full-penetration welds if the weld metal has a lower fraction solid than the PMZ throughout PMZ solidification.

7) *Opposite effects of filler metals 5356 and 4043 on cracking*: The long recognized opposite effects of filler metals 5356 and 4043 on liquation cracking in 6000-series alloys can now be explained. Filler 5356 can make the solidifying and contracting weld metal higher in f_S than the PMZ that it pulls during PMZ terminal solidification, thus encouraging it to tear the PMZ. On the contrary, filler 4043 can keep the weld metal lower in f_S throughout PMZ solidification.

8) *Liquation cracking in multipass welds of thick plates:* The T-f_S curves show that Al-Mg filler metals such as 5356 and NG61 are likely to cause liquation crack-

ing in full-penetration welds in thin sheets of 6000-series aluminum alloys such as 6061 and 6082, where the dilution levels are higher (50–90%), but much less likely to do so in multipass welds in thick plates, where the dilution levels are lower (10–40%). However, bands of solute segregation through the thickness of thick plates can cause local decreases in f_S in the PMZ, resulting in weld-metal f_S > PMZ f_S and hence liquation cracking in the PMZ along the bands.

9) *Necessary conditions for liquation cracking in Al-Cu welds*: The necessary condition for liquation cracking in full-penetration Al-Cu welds is a special case of the one proposed here for Al-Mg-Si welds. Since the T-f_S curves for Al-Cu welds are essentially parallel to one another without any intersections, a higher f_S in the weld metal than in the PMZ throughout PMZ solidification is necessary for liquation cracking to occur (Ref. 26). However, weld-metal f_S > PMZ f_S during PMZ terminal solidification includes the special case of weld-metal f_S > PMZ f_S throughout PMZ solidification.

Acknowledgments

This work was supported by National Science Foundation under Grant No. DMR-0098776. The authors are grateful to Bruce Albrecht and Todd Holverson of Miller Electric Manufacturing Co., Appleton, Wis., for donating the welding equipment (including Invision 456P power source, and XR-M wire feeder and gun) and for their technical assistance during our study. The authors thank Prof. Y. A. Chang of University of Wisconsin-Madison for providing the database required for calculating the T-f_S curves. They also thank Dr. Fanyou Xie for helpful discussions.

References

1. Kou S. 2003. *Welding Metallurgy*, 2nd edition, pp. 151, 160–163, and 303–339. New York, N.Y.: John Wiley and Sons.

2. Dudas, J. H., and Collins, F. R. 1966. Preventing weld cracks in high-strength aluminum alloys. *Welding Journal* 45(6): 241-s to 249-s.

3. Metzger, G. E. 1967. Some mechanical properties of welds in 6061 aluminum alloy sheet. *Welding Journal* 46(10): 457-s to 469-s.

4. Steenbergen, J. E., and Thornton, H. R. 1970. Quantitative determination of the conditions for hot cracking during welding for aluminum alloys. *Welding Journal* 49(2): 61-s to 68-s.

5. Gittos, N. F., and Scott, M. H. 1981. Heat-affected zone cracking of Al-Mg-Si alloys. *Welding Journal* 60(6): 95-s to 103-s.

6. Ma, T., and Den Ouden, G. 1999. Liquation cracking susceptibility of Al-Zn-Mg alloys. *International Journal for the Joining of Materials* (Denmark) 11(3): 61–67.

7. Katoh, M., and Kerr, H. W. 1987. Investigation of heat-affected zone cracking of GTA welds of Al-Mg-Si alloys using the Varestraint test. *Welding Journal* 66(12): 360-s to 368-s.

8. Kerr, H. W., and Katoh, M. 1987. Investigation of heat-affected zone cracking of GMA welds of Al-Mg-Si alloys using the Varestraint test. *Welding Journal* 66(9): 251-s to 259-s.

9. Miyazaki, M., Nishio, K., Katoh, M., Mukae, S., and Kerr, H. W. 1990. Quantitative investigation of heat-affected zone cracking in aluminum Alloy 6061. *Welding Journal* 69(9): 362-s to 371-s.

10. Gitter, R., Maier, J., Muller, W., and Schwellinger, P. 1992. Formation and effect of grain boundary openings in AlMgSi alloys caused by welding. *Proceedings of 5th International Conference on Aluminum Weldments*. P. 4.1.1. Eds. D. Kostcas, R. Ondra, and F. Ostermann, Technische Universita Munchen, Munchen, Germany.

11. Powell, G. L. F., Baughn, K., Ahmed, N., Dalton, J. W., and Robinson, P. 1995. The cracking of 6000 series aluminum alloys during welding. *Proceedings of International Conference on Materials in Welding and Joining*. Institute of Metals and Materials Australasia, Parkville, Victoria, Australia.

12. Ellis, M. B. D., Gittos, M. F., and Hadley, I. 1997. Significance of liquation cracks in thick section Al-Mg-Si alloy plate. *The Welding Institute Journal* (U.K.) 6(2): 213–255.

13. Schillinger, D. E., Betz, I. G., Hussey, F. W., and Markus, H. 1963. Improving weld strength in 2000 series aluminum alloys. *Welding Journal* 42: 269-s to 275-s.

14. Young, J. G. 1968. BWRA experience in the welding of aluminum-zinc-magnesium alloys. *Welding Journal* 47(10): 451-s to 461-s.

15. Lippold, J. C., Nippes, E. F., and Savage, W. F. 1977. An investigation of hot cracking in 5083-O aluminum alloy weldments. *Welding Journal* 56(6): 171-s to 178-s.

16. Huang, C., Kou, S., and Purins, J. R. 2001. Liquation, solidification, segregation and hot cracking in the partially melted zone of Al-4.5Cu welds. *Proceedings of Merton C. Flemings Symposium on Solidification Processing*. p. 229. Eds. R. Abbaschian, H. Brody, and A. Mortensen, The Mineral, Metals and Materials Society, Warrendale, Pa.

17. Huang, C., and Kou, S. 2000. Partially melted zone in aluminum welds – liquation mechanism and directional solidification. *Welding Journal* 79 (5): 113-s to 120-s.

18. Huang, C., and Kou, S. 2002. Liquation mechanism in welds of multicomponent aluminum alloys. *Welding Journal* 81 (10): 211-s to 222-s.

19. Huang, C., and Kou, S. 2001. Partially melted zone in aluminum welds – planar and cellular solidification. *Welding Journal* 80 (2): 46-s to 53-s.

20. Huang, C., and Kou, S. 2001. Partially melted zone in aluminum welds – solute segregation and mechanical behavior. *Welding Journal* 80 (1): 9-s to 17-s.

21. Borland J. C., and Rogerson, J. H. 1963. Examination of the patch test for assessing hot cracking tendencies of weld metal. *British Welding Journal* 8: 494–499.

22. Savage, W. F., and Lundin, C. D. 1965. The Varestraint test. *Welding Journal* 44(10): 433-s to 442-s.

23. Savage, W. F., and Lundin, C. D. 1966. Application of the Varestraint technique to the study of weldability. *Welding Journal* 45(11): 497-s to 503-s.

24. Huang, C., and Kou, S. 2003. Liquation cracking in partial-penetration aluminum welds: Effect of penetration oscillation and backfilling. *Welding Journal* 82(7): 184-s to 194-s.

25. Huang, C., Cao, G., and Kou, S. Liquation cracking in partial-penetration aluminum welds: Assessing tendencies to liquate, crack and backfill. *Science and Technology of Welding and Joining*, in press.

26. Huang, C., and Kou, S. 2004 Liquation cracking in full-penetration Al-Cu welds. *Welding Journal* 83(2): 50-s to 58-s.

27. Cross, C. E., and Gutscher, D. 2003. Effect of Cu and Fe on weldability of aluminum 2519. In *Trends in Welding Research*, ASM International, Materials Park, Ohio, ed. by S.A. David et al., pp. 638–641.

28. Nelson, T. W., Lippold, J. C., Lin, W., and Baselack III, W. A. 1997. Evaluation of the circular patch test for assessing weld solidification cracking, I. Development of a test method. *Welding Journal* 76(3): 110-s to 119-s.

29. Houldcroft, R. T. 1954. Dilution and uniformity in aluminum alloy weld beads. *British Welding Journal* 1: 468–472.

30. Woods, R. A., 1980. Metal transfer in aluminum alloys. *Welding Journal* 59(2): 59-s to 66-s.

31. Flemings, M. C. 1974. *Solidification Processing*, pp. 34–36, 160–162, and Appendix B. New York, N.Y.: McGraw-Hill.

32. Philips, H. W. L. 1959. *Annotated Equilibrium Diagrams of Some Aluminum Alloy Systems*. p. 67. Institute of Metals, London, U.K.

33. *Pandat*. 2001. Phase diagram calculation software package for multicompouent systems. 2001. CompuTherm LLC, Madison, Wis.

34. *PanAluminum* 2001. Thermodynamic database for commercial aluminum alloys. CompuTherm LLC, Madison, Wis.

35. Liu, Z. K., and Chang, Y. A. 1999. Thermodynamic assessment of the Al-Fe-Si system. *Metallurgical and Materials Transactions A* 30A(4): 1081–1095A.

36. Liang, H., and Chang, Y. A. 1999. A thermodynamic database on aluminum alloys for practical alloy design. *Light Metals*, Minerals, Metals and Materials Society/AIME, pp. 875–881.

37. Chang, Y. A., Xie, F. Y., Kraft, T., Zuo, Y., and Moon, C. H. 1999. Microstructure and microsegregation in Al-rich Al-Cu-Mg alloys. *Acta Materialia* 47(2): 489-500.

38. Huang, W., and Chang, Y. A. 1998. A thermodynamic analysis of the Al-Re system.

Journal of Phase Equilibria 19(4): 361–366.

39. Liang, H., and Chang, Y. A. 1998. A thermodynamic description for the Al-Cu-Zn system. *Journal of Phase Equilibria* 19(1): 25–37.

40. Liang, H., Chen, S. L., and Chang, Y. A. 1997. A thermodynamic description of the Al-Mg-Zn system. *Metallurgical and Materials Transactions* A 28A(9): 1725–1734A.

41. Chen, S. L., Zuo, Y., Liang, H., and Chang, Y. A. 1997. A thermodynamic description for the ternary Al-Mg-Cu system. *Metallurgical and Materials Transactions* A 28A(2): 435–446A.

42. Zuo, Y., and Chang, Y. A. 1996. Calculation of phase diagram and solidification paths of ternary. *Materials Science Forum* 215–216: 141–148.

43. Chang, Y. A., Chen, S. L., Zuo, Y., Zhang, F., Daniel, S. L., Moon, C. H., Liang, H., Xie, F. Y., Huang, W., and Liu, Z. K. 1996. Phase diagram calculation: a critical tool for alloy and processing design. *Proceedings of The International Conference-MSMM'96. Modeling and Simulation in Metallurgical Engineering and Materials Science*, Metallurgical Industry Press, pp. 185–190.

44. Chen, S. L., and Chang, Y. A. 1993. A thermodynamic analysis of the Al-Zn system and phase diagram calculation. *Calphad* 17(2): 113–124.

45. Zuo, Y., and Chang, Y. A. 1993. Thermodynamic calculation of the aluminum-magnesium phase diagram. *Calphad* 17(2): 161–174.

46. Zuo, Y., and Chang, Y. A. 1992. Calculation of Phase Diagram and Solidification Paths of Aluminum-Rich Al-Mg-Cu Ternary Alloys. The Minerals, Metals & Materials Society, pp. 935–942.

47. Chen, S. W., Beumler, H. W., and Chang, Y. A. 1991. Experimental determination of the phase equilibria of aluminum-rich Al-Li-Cu alloys. *Metallurgical Transactions* A 22A(1): 203–213.

48. Chen, S. W., and Chang, Y. A. 1991. Application of thermodynamic models to the calculation of solidification paths of aluminum-rich Al-Li alloys. *Metallurgical Transactions* A 22A(1): 267–271.

49. Chen, S. W., Lin, J. C., Chang, Y. A., and Chu, M. G. 1990. Phase Equilibria and Solidification of Aluminum-Rich Al-Li-Cu Alloys. The Minerals, Metals & Materials Society, pp. 985–988.

50. Chen, S. W., Jan, C. H., Lin, J. C., and Chang, Y. A. 1989. Phase equilibria of the Al-Li binary system. *Metallurgical Transactions* A 20A(11): 2247–2258.

51. Chen, S. W., Chang, Y. A., and Chu, M. G. 1989. *Phase Equilibria and Solidification of Al-Li Alloys*. Materials and Component Engineering Publications Ltd., pp. 585–594.

52. Singer, A. R. E., and Cottrell, S. A. 1946. Properties of the Al-Si alloys at temperatures in the region of the solidus. *Journal of Institute of Metals* 73: 33–54.

53. Jennings, P. H., Singer, A. R. E., and Pumphrey, W. I. 1948. Hot-shortness of some high-purity alloys in the systems aluminum-copper-silicon and aluminum-magnesium-silicon. *J. Inst. Metals* 74: 227–248.

Preparation of Manuscripts for Submission to the *Welding Journal* Research Supplement

All authors should address themselves to the following questions when writing papers for submission to the Welding Research Supplement:

- Why was the work done?
- What was done?
- What was found?
- What is the significance of your results?
- What are your most important conclusions?

With those questions in mind, most authors can logically organize their material along the following lines, using suitable headings and subheadings to divide the paper.

1) **Abstract.** A concise summary of the major elements of the presentation, not exceeding 200 words, to help the reader decide if the information is for him or her.

2) **Introduction.** A short statement giving relevant background, purpose, and scope to help orient the reader. Do not duplicate the abstract.

3) **Experimental Procedure, Materials, Equipment.**

4) **Results, Discussion.** The facts or data obtained and their evaluation.

5) **Conclusion.** An evaluation and interpretation of your results. Most often, this is what the readers remember.

6) **Acknowledgment, References and Appendix.**

Keep in mind that proper use of terms, abbreviations, and symbols are important considerations in processing a manuscript for publication. For welding terminology, the *Welding Journal* adheres to AWS A3.0:2001, *Standard Welding Terms and Definitions.*

Papers submitted for consideration in the Welding Research Supplement are required to undergo Peer Review before acceptance for publication. Submit an original and one copy (double-spaced, with 1-in. margins on 8 ½ x 11-in. or A4 paper) of the manuscript. A manuscript submission form should accompany the manuscript.

Tables and figures should be separate from the manuscript copy and only high-quality figures will be published. Figures should be original line art or glossy photos. Special instructions are required if figures are submitted by electronic means. To receive complete instructions and the manuscript submission form, please contact the Peer Review Coordinator, Doreen Kubish, at (305) 443-9353, ext. 275; FAX 305-443-7404; or write to the American Welding Society, 550 NW LeJeune Rd., Miami, FL 33126.